Journal of Power Sources 222 (2013) 503–509

Contents lists available at SciVerse ScienceDirect

Journal of Power Sources

journal homepage: www.elsevier.com/locate/jpowsour

Silicon composite thick film electrodeposited on a nickel micro-nanocones hierarchical structured current collector for lithium batteries

Tao Hang [a], Hiroki Nara [a], Tokihiko Yokoshima [a], Toshiyuki Momma [b], Tetsuya Osaka [b,*]

[a] Research Institute for Science and Engineering, Waseda University, 3-4-1 Okubo, Shinjuku, Tokyo 169-8555, Japan
[b] Department of Applied Chemistry, Faculty of Science and Engineering, Waseda University, 3-4-1 Okubo, Shinjuku, Tokyo 169-8555, Japan

HIGHLIGHTS

- Micro-nanocones hierarchical structure (MHS) was fabricated by electrodeposition.
- Si composite thick film was electrodeposited on MHS current collector.
- The MHS supported Si anode demonstrated outstanding Li^+ storage properties.
- The unique architecture of MHS and porous Si film favor a stable cycling behavior.

GRAPHICAL ABSTRACT

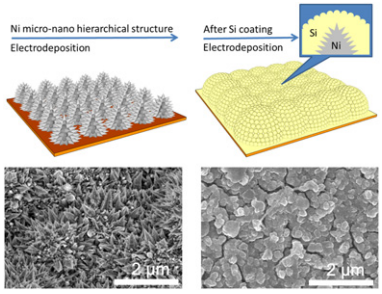

ARTICLE INFO

Article history:
Received 26 May 2012
Received in revised form
31 August 2012
Accepted 3 September 2012
Available online 11 September 2012

Keywords:
Si anode
Thick film
Electrodeposition
Micro-nanocones hierarchical structure
Current collector
Lithium battery

ABSTRACT

Electrodeposition methods were developed for the fabrication of Si composite anodes with nickel micro-nanocones hierarchical structure (MHS) current collectors for Li secondary batteries. This unique structured nickel current collector is electrodeposited in a simple process to create a complex high surface area conductive substrate, as well as to enhance the interfacial strength between active materials and substrate during cyclic lithiation/delithiation. The MHS supported Si composite anode demonstrated outstanding Li^+ storage properties with reversible capacity over 800 mAh g^{-1} (600 μAh cm^{-2}) after 100th cycle with superior retention of 99.6% per cycle. The improved performance of nickel MHS supported Si thick films indicate the potential for their application as electrode materials for high performance energy storage.

1. Introduction

It is essential to develop Li-ion batteries with higher storage capacity, greater cycling stability, higher power and faster charging rate for next-generation electrical vehicles [1–5]. Silicon has been targeted to replace carbon as one of the most promising anode materials owing to its high theoretical specific capacity (4200 mAh g^{-1}, 10 times that of commercial graphite anodes), high volumetric capacity (9786 mAh cm^{-3}), and low charge/discharge voltage [6–10]. However, silicon experiences a large volume change due to the lithiation/delithiation process during charge–discharge cycles, which leads to severe silicon particle pulverization and loss of contact with the current collector [11,12]. This mechanical disintegration and electronic degradation thereby triggered drastic capacity fading and have hindered the practical implementation of Si anodes.

* Corresponding author. Tel.: +81 3 5286 3202; fax: +81 3 3205 2074.
E-mail address: osakatets@waseda.jp (T. Osaka).

0378-7753/$ – see front matter © 2012 Elsevier B.V. All rights reserved.
http://dx.doi.org/10.1016/j.jpowsour.2012.09.008

In our previous study, a novel Si composite film was developed for Li battery anodes by electrodeposition from an organic solvent [13,14]. The electrodeposition method was introduced based on the assumption that, to form a Si containing anode from an organic solution, the composite of Si with an organic/inorganic compound withstands the stress during the anode operation. This film, several microns thick, performed as a Li battery anode with a discharge capacity of ca. 1000 mAh g^{-1} of Si at 2000 cycle and ca. 800 mAh g^{-1} even at 7000 cycle, which substantially improved electrochemical performance both in specific capacity and cycle ability.

Despite the excellent performance of the proposed Si composite anode, a much thicker film is required to provide sufficient capacity for matching the cathode material of commercialized Li batteries. However, increasing the thickness of the Si composite films seriously affected its electrochemical behavior, because of the poor electron conductivity of the active material and the weak adhesion strength between the thick film and the current collector.

To circumvent these issues, one way is to use a gas deposition method to form a thick film with very strong adhesion between the particles as well as between the active materials and the substrate [15]. Another efficient way is to design a specific structured substrate with high roughness to improve adhesive properties between active materials and current collector [16]. Kim et al. demonstrated that a Cu current collector with a properly modified surface morphology efficiently enhanced the electrochemical performance of a Si-based anode [17]. Uehara et al. introduced a 1.1 μm thick silicon film deposited on a well-etched substrate maintained specific capacity over 1500 mAh g^{-1} even after 400 cycles [18]. However, these methods have some disadvantages such as comparatively complicated procedures, and high synthesis costs.

Recently, we have developed a unique nickel micro-nanocones hierarchical structure (MHS) fabricated by a simple and economical electrodeposition method with a crystallization modifying agent. This unique structure has been once reported for its superhydrophobic performance [19]. In this paper, we introduce this Ni MHS as the current collector to support the electrodeposited Si composite thick film anode for Li battery, and demonstrate that this MHS substrate plays an important role in maintaining high performance in the thick film anode.

Fig. 1 illustrates a typical architecture and preparation procedure of this MHS supported Si composite electrode. The design includes large surface area Ni MHS as the inactive confining buffer to accommodate the volume variation as well as the structural support to enhance the adhesion strength between the active materials and current collectors. Subsequently, an Si composite thick film is electrodeposited from an organic solvent on the Ni MHS substrate as the electrochemically active material for lithium-ion storage. The Ni MHS supported Si composite anodes exhibit a relatively high reversible capacity of around 800 μAh cm^{-2} (1000 mAh g^{-1}) with 88% capacity retention over 300 cycles.

2. Experimental

The nickel MHS films were electroplated onto commercial pure Cu foils. The Cu foils were anodized at 0.25 A cm^{-2} in a solution containing 10 g l^{-1} KOH, 10 g l^{-1} santomerse, and 70 g l^{-1} deoil powder for 30 s and acid-cleaned with 10% HCl for another 10 s before electroplating. The electrodeposition solution was composed of analytical pure $NiCl_2 \cdot 6H_2O$ (providing Ni ions) 1 mol L^{-1}, H_3BO_3 (pH buffer) 0.5 mol L^{-1}, and crystal modifier (ethylenediamine dihydrochloride) 1.5 mol L^{-1} dissolved in deionized water. The temperature of the deposition solution was kept at 60 °C and pH value was 4.0. The deposition current density was varied from 0.5 A dm^{-2} to 5.0 A dm^{-2} .The deposition time was also controlled to obtain micro-nanocones of different size. The hierarchical structure Ni film was produced by two steps. First, a layer of microcones array was deposited at a relatively lower current density of 0.5 A cm^{-2} for 20 min. After that, nanocones were deposited onto the surface of the microcones at a higher current density of 5.0 A cm^{-2} for 1 min to form an MHS. This two-step process provides flexibility in the fabrication of a variety of hierarchical structures. The MHS substrate was then rinsed with distilled water, dried in vacuum overnight, and transferred into an Ar atmosphere.

For electrodeposition of the Si composite, the electrolytic solution containing 0.5 mol dm^{-3} $SiCl_4$ (Sigma–Aldrich) and 0.5 mol dm^{-3} tetrabuthylammonium perchlorate in propylene carbonate (TBAP, Kanto Chemical/PC, Kishida, H_2O content less than 30 ppm) was prepared in dry air with dew point below −50 °C. The electrochemical cell equipped with a Li/Li^+ reference electrode, 1.0 cm^2 MHS on the Cu foil as a working electrode, and Pt counter electrode was set up in Ar atmosphere with dew point lower than −100 °C. A constant cathodic current of 1.0 mA cm^{-2} was applied to pass a charge of 2–20 C cm^{-2} for the deposition. The deposit on the MHS substrate was then transferred into an electrochemical cell containing 1.0 mol dm^{-3} lithium perchlorate ($LiClO_4$) in PC − ethylenecarbonate (EC) (1:1 v/v) electrolyte solution (Kishida, H_2O content less than 20 ppm), and reduced by constant-current–constant-voltage mode with 500 μA cm^{-2} and 0.01 V vs. Li/Li^+ for 10 h.

Electrochemical performance of the resultant composite as an anode of a Li battery was characterized by a constant current charge–discharge test with 500 μA cm^{-2} in the potential range

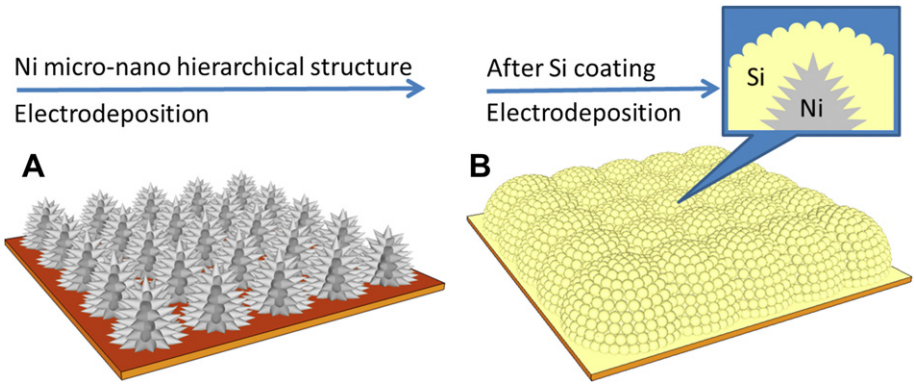

Fig. 1. Schematic diagram illustrating the fabrication of a nickel nanocone-array supported silicon anode architecture: (A) nickel micro-nanocones hierarchical structure: (B) after silicon composite electrodeposition.

between 0.01 V and 1.20 V vs. Li/Li^+. The gravimetric capacity of the Si-based composite electrode was calculated according to the weight of silicon in the composites obtained from inductively coupled plasma (ICP) analysis. Cyclic voltammogram (CV) of the electrode was measured in the range of 0.01–1.20 V vs. Li/Li^+ at a scan rate of 0.10 mV s^{-1}. Electrochemical impedance spectra (EIS) were taken with a Solartron 1400 over the frequency range from 1 MHz to 0.01 Hz with ac amplitude of 10 mV.

The surface morphologies of the MHS current collector and the Si composite film were observed by means of field emission scanning electron microscopy (FE-SEM, Hitachi, S-4800). The FE-SEM also offers the ability to obtain energy dispersive X-ray spectroscopy (EDX) for surface elemental analysis of the samples. The cross sectional elemental analysis is conducted by X-ray photoelectron spectroscopy (XPS, JEOL, JPS-9010TR). The crystal structures of the products were identified by X-ray diffraction (XRD, RINT-Ultima III).

3. Results and discussion

Fig. 2a shows a typical scanning electron microscopy (SEM) image of the micro-nano hierarchical structure Ni film synthesized by two-step electrodeposition. It is clear that microflower-like protrusions with a diameter in the range of 3 μm are formed. The enlarged view of a single microflower (inset of Fig. 2a) reveals that for each microflower, many nanocones were dispersed randomly. The average height of the cones and the mean diameter of their roots are approximately 300 nm and 200 nm, respectively. The tips of the cones are very sharp, corresponding to an apex angle of ~ 30°. The growth process of the MHS was template-free, which was somewhat different from the traditional nanostructure growth method with ordered templates. Therefore, the nickel MHS are not very regular and uniform. Larger and smaller cones are also observed in the mix. Compared with the nano-size hierarchical Ni film we reported for superhydrophobic properties [19], which consisted of the first layer of 500 nm Ni nanocones and second layer of 50–100 nm Ni protrusions, the micro-scale hierarchical structure in this study allows for thicker deposits of Si composite.

Fig. 2b is the SEM image of the macroscopically homogeneous deposit. The surface morphology of the deposit appears to be uninfluenced by the pattern of MHS substrate, which may due to the greater thickness of the deposit relative to the size of MHS. The enlarged SEM image of Fig. 2b indicates that the deposit consisted of sub-micrometer clusters covering the MHS substrate with voids. This porous structure maybe related to the gas bubbles arising from the reductive decomposition of PC solvent on the surface of the electrode [20]. A small amount of mini-bubbles can be observed carefully on the cathode during the experiment.

The existence of elemental silicon was confirmed by SEM-EDX (Fig. 3a). The elemental mapping shows that Si, O, C and Cl were distributed homogeneously at the nanometric scale (not shown), while a small amount of Ni can also be detected because of the existence of voids in the Si film. The XPS depth profiles of the elements of Si, C, O, and Cl in the deposit obtained by the electrodeposition of silicon are shown in Fig. 3b. The approximate sputtering rate was around 0.1 μm min^{-1}. The silicon and oxygen content were found to increase with depth near the surface, and saturate at ca. 35 at.% and ca. 40 at.%. The carbon and chlorine contents were found to decrease with depth near the surface from ca. 40 at.% and ca. 10 at.%, to ca. 20 at.% and ca. 0 at.%, respectively. These tendencies near the surface are attributed to the post-processing of the sample after electrodeposition. The composition near the surface was considered as residual PC and $SiCl_4$ after post-processing. The results of XPS (not shown here) also indicate that the deposit was composed of Si existing in an oxidized state and decomposition products of the organic electrolyte. The oxidation state of Si is deduced to be SiO in our previous report [13]. However, it could also be considered as the metal Si covered by SiO_2. Further investigation needs to be carried out to confirm the oxidation state of Si in our future work.

The crystallinity of the deposits formed by the electrodeposition of silicon before and after 100 charge–discharge cycles was investigated by XRD (shown in Fig. 3c). Peaks observed correspond to Ni and Cu. These peaks are due to the Ni MHS and the Cu foil substrate. Peaks expected for silicon, which are indicated in Fig. 3c by dotted lines, were not observed. This result suggests that the deposit formed by the electrodeposition of silicon was in an amorphous or nano-crystalline state and its structure can be maintained during cycling.

The lithium insertion/extraction reaction of the MHS supported Si composite anode was investigated by cyclic voltammogram (CV). Fig. 4a shows typical CV curves of the MHS before and after Si deposition over the potential window of 0.01–1.2 V at a scan rate of 0.1 mV s^{-1}. Before the electrodeposition of Si, the CV curve shows double layer capacitor behavior and no peak related to lithiation of MHS/Cu is observed, which indicates the inactive nature of the Ni MHS. After Si deposition, the CV curve changes shape dramatically and peaks related to lithiation/delithiation of Si are observed. The peak at 0.1 V in the cathodic branch is due to the reaction of a-Si to an amorphous Li_xSi phase. The two peaks at 0.40 and 0.55 V in the anodic branch correspond to delithiation of a-Li_xSi to a-Si [21].

Fig. 4b shows the discharge–charge curves of the MHS supported Si composite anode. The sloped discharge and charge trends confirm its amorphous structure. The lithiation and delithiation take place in a voltage range of 0.30–0.01 V and 0.10–0.65 V vs. Li/Li^+, respectively, which is consistent with the result from CV (Fig. 4a). The first litiation capacity is over 1239 mAh g^{-1} (743.6 μAh cm^{-2}), and the first delitiation capacity is 1182 mAh g^{-1} (709.7 μAh cm^{-2}), educing a first cycle coulombic efficiency of 95%.

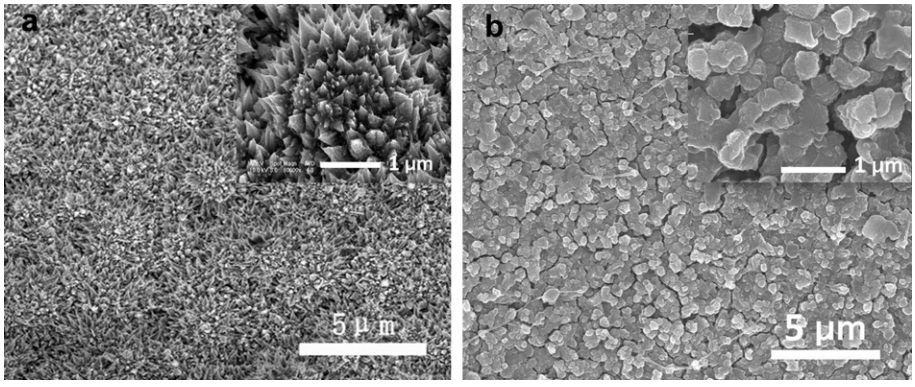

Fig. 2. SEM images of (a) electrodeposited Ni micro-nano hierarchical structure substrate, and (b) Silicon composites deposited on an MHS substrate.

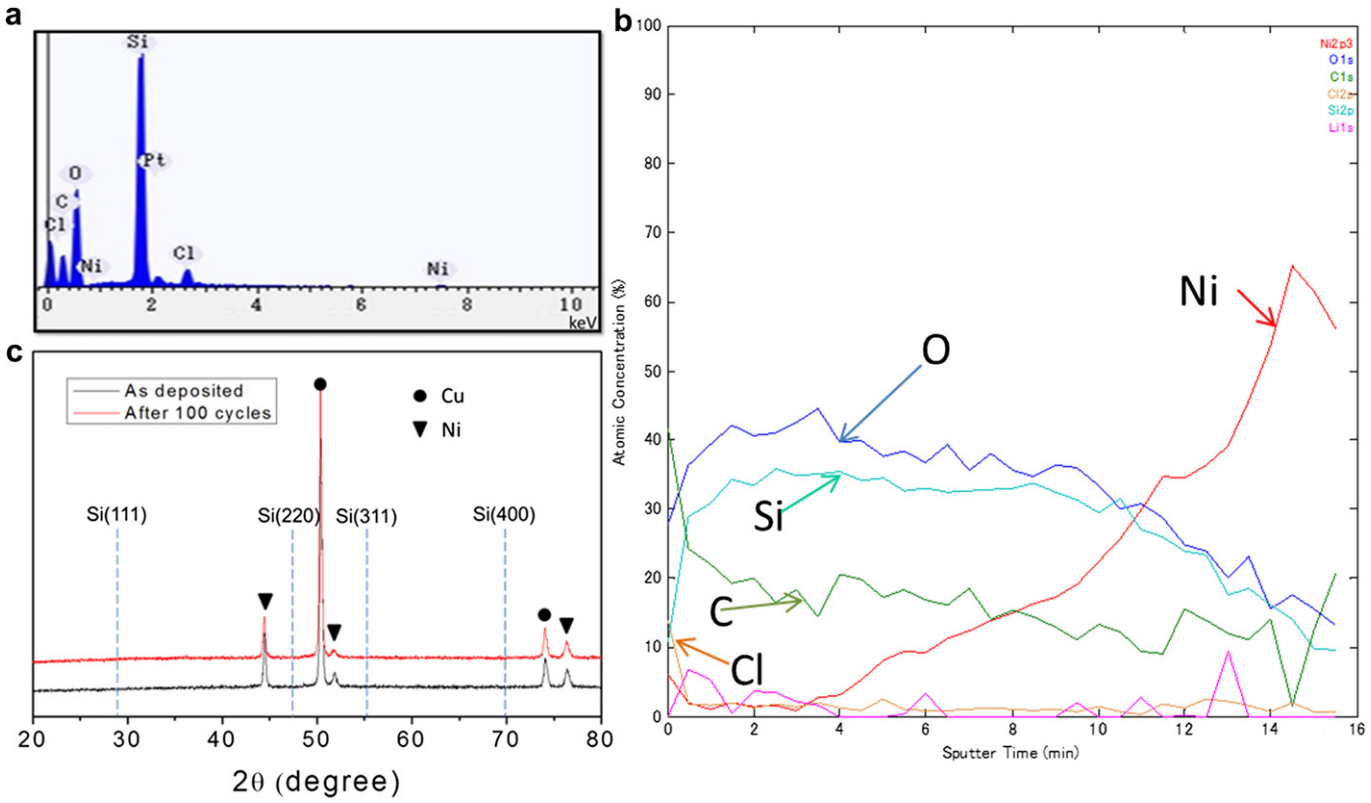

Fig. 3. (a) SEM-EDX spectroscopy, (b) XPS depth profile, and (c) XRD patterns of Si thick film deposited on Ni MHS substrate before and after cycling.

The cycling performance of the MHS supported Si composite anodes with different quantities of electricity for electrodeposition (amount of deposits) is compared in Fig. 5a. The use of gravimetric units for evaluating the capacity of such thick film could generate more or fewer errors. For accuracy and convenience, geometric units are used here for comparison. The thickness of the Si film was calculated by the charge used for electrodeposition with the result we measured by TEM in our previous report [14]. The gravimetric capacity of the 12.5 μm thick film (50 coulombs for electrodeposition, specific weight of Si around 0.75 mg) after 100 cycles was around 800 mAh g^{-1}, which was 33% lower than that of the 2 coulombs electrodeposited thin film (specific capacity around 1200 mAh g^{-1} after 100 cycles). However, comparing these curves shows that the cycling performance is not almost influenced by the thickness (amount of deposits per square centimeter) of the Si composite layer. All the deposited films show very good capacity retention. Even at the thickness of 12.5 μm, the Si composite anode kept a relative stable capacity of 600 μAh cm^{-2} for a long-term run. The capacity loss rate is calculated to be 0.4% per cycle between 1 and 100 cycles. According to the recent reports of the Si thin film electrodes, it is known that 1 μm thick Si film could maintain a capacity of 3000 mAh g^{-1} only within 12 cycles, and 1.2 μm thick Si films gave a capacity of 1000 mAh g^{-1} but a poor cycling ability after the first three cycles [22,23]. The MHS supported Si composite thick film electrode fabricated in this work exhibits significant improvement in cycling stability.

Fig. 5b further shows the influence of the charge–discharge current density on the capacity retention. With the increased current density, the capacity decreases regularly. The reversible capacity decreases from 1100 mAh g^{-1} at the current density of

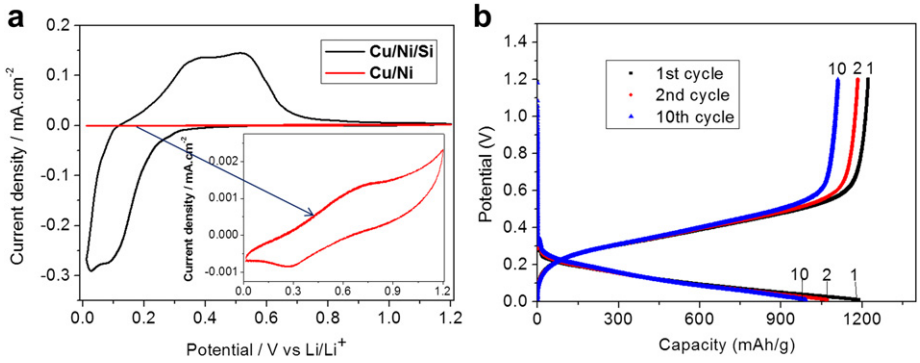

Fig. 4. (a) Typical cyclic voltammogram curve comparison of the MNHS before and after Si deposition at a scan rate of 0.1 mV s^{-1}. (b) Potential profile of MNHS supported Si composite anode for Li battery during constant current charge–discharge cycling. Capacity value was normalized with the weight of Si in the deposit. Applied current density was 250 μA cm^{-2} (0.1-C rate).

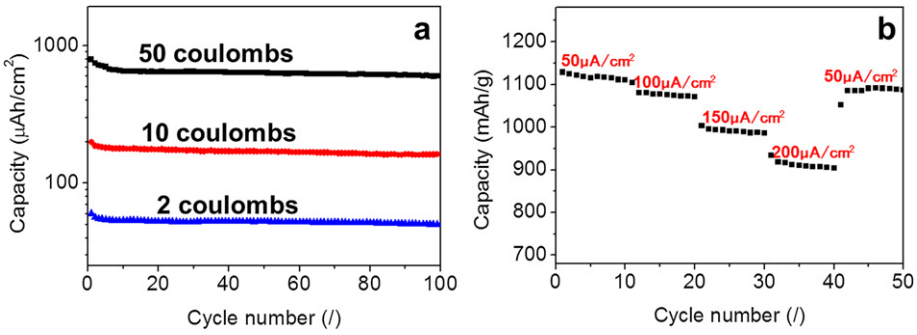

Fig. 5. (a) The cycling performance of the Si film electrodes with different quantities of electricity for Si electrodeposition and (b) the reversible capacities during continuous cycling at various current densities.

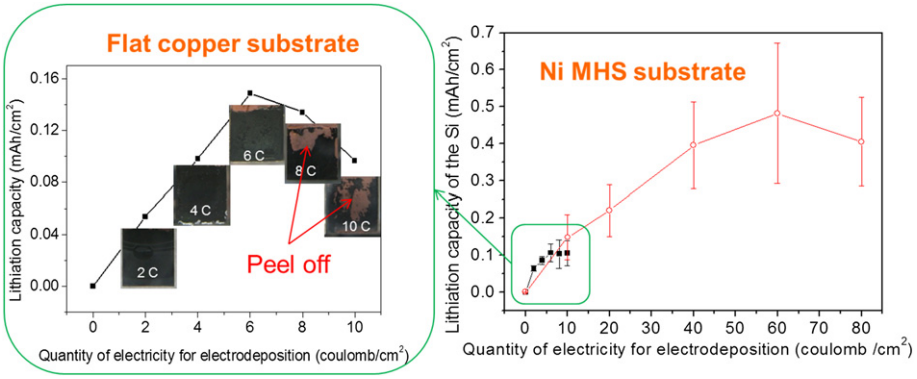

Fig. 6. The geometric capacity of the Si composite film deposited on flat Cu substrates and MHS substrate vs. the charge used for electrodeposition.

50.0 μA cm^{-2} to 900 mAh g^{-1} at the current density of 200 μA cm^{-2}. Moreover, the capacity can be recovered when the current density returns to 50.0 μA cm^{-2}, indicating that the Ni MHS supported Si anode electrode has a good electrochemical reversibility and structural integrity.

Fig. 6 compares the discharge capacities of the Si composite anode deposited on smooth copper substrates and MHS substrate. The Si composite electrode electroplated on the smooth Cu substrate reached the highest reversible capacity of around 150 μAh cm^{-2} (10th cycle) with an electrodeposition charge of 6 C cm^{-2} (specific weight of Si around 0.15 mg). In contrast, the Si composite anode electroplated on the Ni MHS substrate could reach 700 μAh cm^{-2} (10th cycle) at a specific weight of Si around 0.8 mg, which is significantly higher compared to the Si electrodes on flat Cu substrates. It's clearly shown in Fig. 6 that the active materials were peeling off from the Cu substrate when the film thickness was higher than ca. 2 μm (electrodeposition charge of 6 C cm^{-2}), which indicates weak adhesion strength between the Si composite and the flat Cu substrate. It has been reported that the Ni nanostructured substrate is very effective in increasing the adhesion strength between the epoxy molding compound and the Pd pre-plated lead-frame in electronics packaging by a mechanical inter-locking effect [24]. Therefore, the enhanced adhesion strength between the Si composite electrode and the MHS substrate may contribute to the observed improvement in both specific capacity and cycle performance.

Fig. 7 shows the impedances of the electrodeposited silicon composite with different thickness on a Ni MHS current collector after 100 cycles. The impedances were measured upon reaching a full charge at 0.01 V vs. Li/Li^+. All the impedance spectra have similar features: a high-to-medium frequency asymmetric and depressed semicircle and an inclined low frequency line, a behaviour that is in good agreement with previously reported impedance spectra of silicon nanowires [25]. The depressed semicircles would suggest the variation of time constant for the impedance responses including the interfacial reaction of these electrodes. The inclined line in the low-frequency region represents the lithium diffusion impedance. The magnitude of semicircles decreased with increasing the deposition charge. This finding illustrate that the increase of deposition charge does not make the deposited film thicker with keeping the surface area contacting with the electrolyte, but enlarges the reaction surface for the electrochemical reaction. It would be considered that the relatively high ionic and

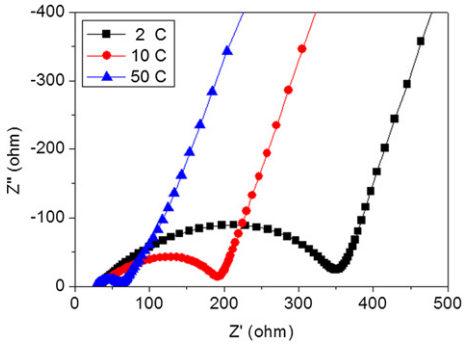

Fig. 7. Nyquist plots of MHS substrate supported Si composite films with different quantities of electric charge for Si electrodeposition.

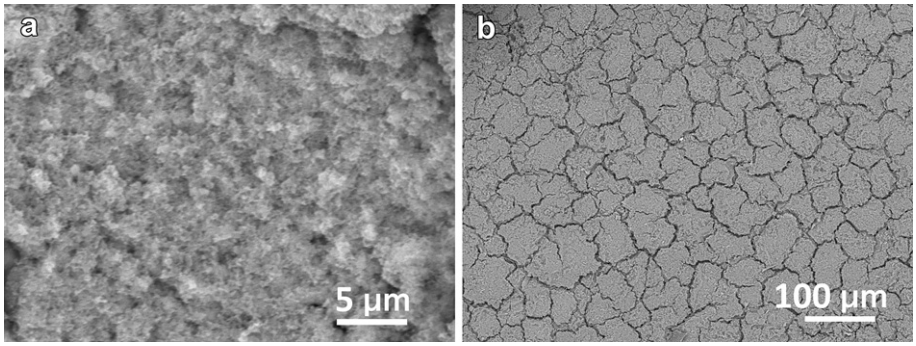

Fig. 8. SEM images of Si composite electrodes (20 coulomb of charge for Si electrodeposition) after 100 cycles in (a) high magnification and (b) low magnification.

electric conductivity in the Si composite thick film enable not only the active material on the surface but also the active material in the thick film to be electrochemically active. Consequently, the charge transfer resistance was decreased because of the increase of the active surface area with thickness increase of the Si composite film. In order to analyse the impedance responses of this material, more detailed analysis on this Si deposit is required. We have proposed the analysing protocol of such asymmetric and depressed semi-circles shown in the Nyquist plots with equivalent circuit based on the electrochemical modelling [26]. SEI is one of the potential component for the understanding of the electrochemical impedance response of anode, while detailed characterization of matrix and interface of Si deposit is essential for taking account into the equivalent circuit for analysis, since the sub-reactions under the cathodic potential at the surface of Si deposit, which was also formed by electrochemical cathodic reaction in organic solution, was not cleared yet.

To further illustrate why the excellent cycle ability of this thick film anode was achieved, the morphology of the MHS supported 10 μm Si film anode was examined by SEM after 100 cycles as shown in Fig. 8. Because of the volume change during lithium insertion/extraction and the formation of SEI layer, the original microspheres feature disappears from the surface. Instead, the Si composite film presents a rough and porous morphology. Cracking of the Si film in a width of ca. 3 μm and length of ca. 30 μm is revealed in a low magnification image. This is regarded as the main cause of the capacity decrease. However, the cracked thick film has not disintegrated and degraded with the Ni MHS sticking to the active materials tightly. It is suggested that that the excellent cycling performance of this electrode with the MHS should be attributed to the maintenance of electric contact between the Si layer and the current collector during cycling. This proves the advantage of this well-designed nickel MHS supported Si composite electrode over the previously reported Si-based anode with nodule-type substrate [17].

4. Conclusions

In summary, a micro-nano hierarchical structure supported silicon composite film was fabricated by electrodeposition as the anode material for Li-ion batteries. The nickel MHS serves as current collector to enhance the adhesion strength between the active materials and substrate and relieve the huge interfacial strains induced by volume expansion. Furthermore, the particular Si composite film morphology with porous particle structure can also buffer the volume change during the lithium insertion/extraction process and favor a stable cycling behavior. This nickel MHS supported Si composite anode exhibited impressive lithium storage capability at 0.2 C rates. The reversible capacity for the first cycle was 1239 mAh g^{-1} (743.6 μAh cm^{-2}), and for the 100th cycle was over 800 mAh g^{-1} (600 μAh cm^{-2}), delivering good retention rate of 99.6% per cycle. This novel anode architecture provides a simple and robust means to produce lithium-ion-based anodes with improved performance, stability, and rate capability. The proposed approach with a very facile procedure may be also exploited for other active materials to achieve a high-capacity and durable electrode for Li-ion batteries.

Acknowledgments

This work was supported by “Research & Development Initiative for Scientific Innovation of New Generation Batteries” from the New Energy and Industrial technology Development Organization of Japan and a Grant-in-Aid for Specially Promoted Research “Establishment of Electrochemical Device Engineering” from the Ministry of Education, Culture, Sports, Science and Technology, Japan.

References

[1] J.B. Goodenough, Y. Kim, Chemistry of Materials 22 (2010) 587–603.
[2] D.R. Rolison, L.F. Nazar, MRS Bulletin 36 (2011) 486–493.
[3] J.Y. Huang, L. Zhong, C.M. Wang, J.P. Sullivan, W. Xu, L.Q. Zhang, S.X. Mao, N.S. Hudak, X.H. Liu, A. Subramanian, H.Y. Fan, L.A. Qi, A. Kushima, J. Li, Science 330 (2010) 1515–1520.
[4] X.L. Ji, S. Evers, R. Black, L.F. Nazar, Nature Communications 2 (2011).
[5] H.G. Zhang, X.D. Yu, P.V. Braun, Nature Nanotechnology 6 (2011) 277–281.
[6] Y. Yao, K.F. Huo, L.B. Hu, N.A. Liu, J.J. Ha, M.T. McDowell, P.K. Chu, Y. Cui, ACS Nano 5 (2011) 8346–8351.
[7] B.A. Boukamp, G.C. Lesh, R.A. Huggins, Journal of the Electrochemical Society 128 (1981) 725–729.
[8] J.T. Yin, M. Wada, K. Yamamoto, Y. Kitano, S. Tanase, T. Sakai, Journal of the Electrochemical Society 153 (2006) A472–A477.
[9] T. Song, J.L. Xia, J.H. Lee, D.H. Lee, M.S. Kwon, J.M. Choi, J. Wu, S.K. Doo, H. Chang, W. Il Park, D.S. Zang, H. Kim, Y.G. Huang, K.C. Hwang, J.A. Rogers, U. Paik, Nano Letters 10 (2010) 1710–1716.
[10] S.C. Zhang, Z.J. Du, R.X. Lin, T. Jiang, G.R. Liu, X.M. Wu, D.S. Weng, Advanced Materials 22 (2010) 5378.
[11] X.L. Chen, K. Gerasopoulos, J.C. Guo, A. Brown, C.S. Wang, R. Ghodssi, J.N. Culver, ACS Nano 4 (2010) 5366–5372.
[12] R.A. Huggins, Journal of Power Sources 81 (1999) 13–19.
[13] T. Momma, S. Aoki, H. Nara, T. Yokoshima, T. Osaka, Electrochemistry Communications 13 (2011) 969–972.
[14] H. Nara, T. Yokoshima, T. Momma, T. Osaka, Energy & Environmental Science 5 (2012) 6500–6505.
[15] H. Usui, M. Shibata, K. Nakai, H. Sakaguchi, Journal of Power Sources 196 (2011) 2143–2148.
[16] Z.J. Du, S.C. Zhang, Y.L. Xing, X.M. Wu, Journal of Power Sources 196 (2011) 9780–9785.
[17] Y.L. Kim, Y.K. Sun, S.M. Lee, Electrochimica Acta 53 (2008) 4500–4504.
[18] M. Uehara, J. Suzuki, K. Tamura, K. Sekine, T. Takamura, Journal of Power Sources 146 (2005) 441–444.
[19] T. Hang, A.M. Hu, H.Q. Ling, M. Li, D.L. Mao, Applied Surface Science 256 (2010) 2400–2404.
[20] D. Aurbach, M.L. Daroux, P.W. Faguy, E. Yeager, Journal of the Electrochemical Society 134 (1987) 1611–1620.
[21] J. Li, J.R. Dahn, Journal of the Electrochemical Society 154 (2007) A156–A161.
[22] S. Bourderau, T. Brousse, D.M. Schleich, Journal of Power Sources 81 (1999) 233–236.

[23] J.P. Maranchi, A.F. Hepp, P.N. Kumta, Electrochemical and Solid State Letters 6 (2003) A198–A201.
[24] T. Hang, H.Q. Ling, Z.J. Xiu, M. Li, D.L. Mao, Journal of Electronic Materials 36 (2007) 1594–1598.
[25] R. Ruffo, S.S. Hong, C.K. Chan, R.A. Huggins, Y. Cui, Journal of Physical Chemistry C 113 (2009) 11390–11398.
[26] T. Osaka, T. Momma, D. Mukoyama, H. Nara, Journal of Power Sources 205 (2012) 483–486.